





Numerical investigation of graphene-based efficient and broadband metasurface for terahertz solar absorber

Rajendrasinh Jadeja¹, Shreyas Charola², Shobhit K. Patel^{2,3}, Juveriya Parmar^{2,3},
Mayurkumar Ladumor², Truong Khang Nguyen^{4,5} , and Vigneswaran Dhasarathan^{4,5,*} 

¹Department of Electrical Engineering, Marwadi University, Rajkot, Gujarat 360002, India

²Department of Electronics and Communication Engineering, Marwadi University, Rajkot, Gujarat 360002, India

³Department of Physics, Marwadi University, Rajkot, Gujarat 360002, India

⁴Division of Computational Physics, Institute for Computational Science, Ton Duc Thang University, Ho Chi Minh City, Vietnam

⁵Faculty of Electrical and Electronics Engineering, Ton Duc Thang University, Ho Chi Minh City, Vietnam

Received: 17 October 2019

Accepted: 2 December 2019

Published online:

9 December 2019

© Springer Science+Business Media, LLC, part of Springer Nature 2019

ABSTRACT

Graphene-based efficient metasurface solar absorber is presented. Graphene monolayer sheet is integrated over silicon dioxide dielectric layer to improve the bandwidth and achieve maximum absorption in the visible region from 430 to 770 THz. Simulation results indicate that the average absorption of our graphene-based metasurface absorber is more than 84% in the visible range. The absorber C-shape metasurface top layer placed above the graphene sheet is made up of tungsten material, and bottom layer made up of tungsten material helps in absorbing incoming electromagnetic light. The resonance frequency can be tuned in a wide frequency range by changing different physical parameters of proposed absorbers design. The absorption efficiency results of the proposed design are also compared with previously published similar absorber design to show the improvement of absorption in the proposed design. The proposed design is useful for designing next-generation graphene-based sensors and photovoltaic devices. Purposed graphene-based metasurface absorber can be used as a basic building block of solar energy-harvesting photovoltaic devices.

Introduction

The life on earth is the gift of several resources which is everlasting. These resources we call as natural resources. Natural resources are classified into

renewable and non-renewable resources. The non-renewable energy sources like coal, petroleum, natural gases, etc., are used again and again and can be exhausted one day. Converting one form of energy to electric energy using non-renewable energy sources

Address correspondence to E-mail: vigneswaran.d@tdtu.edu.vn

requires a large area and huge maintenance which increases the overall cost of the project. The renewable energy source like the sun provides clean and safe energy which is inexhaustible in nature and also do not disturb the ecological balance of nature [1]. The earth receives an abundant amount of solar radiation, so it is necessary to design an efficient coating layer which absorbs the maximum region of the solar spectrum (infrared, visible and ultraviolet region). The sun radiation reaches earth, where most of the energy is distributed in the visible and infrared region. Narrowband, multi-band and multilayered light absorber are designed to use as sub-system blocks in the practical applications like sensing [2–4], filtering, thermal emission, etc. [5–8].

The solar absorbers available today have lower efficiency and cannot operate over wide range of frequencies. One of the problems of the current solar absorber is its complex design. This complex design leads to increase the cost of fabrication because of its complexity. Another type of absorber structure is made up of perovskites which has a disadvantage of less durability, less stability and narrowband absorption [9, 10]. Therefore, there is a need to design a solar absorber with artificial materials in the terahertz frequency region. Artificial materials with unusual electromagnetic properties which are not found in nature are called “Metamaterials.” The electromagnetic response mainly depends on the two properties, the electric permittivity and magnetic permeability [11, 12].

Metamaterial absorbers are gaining interest in the researcher community because of their broadband behaviour in the infrared, visible and ultraviolet (UV) regions [13–17]. Metamaterials perfect absorbers for radio to optical frequency range are presented in [13]. Achieving single-band and multi-band absorbers is easy compared to achieving broadband metamaterial absorber. Broadband metamaterial absorber is presented for visible and near-infrared regions [14]. The array of metamaterial gold resonators placed on silicon dioxide (SiO_2) substrate can also give broadband response in 200 THz to 400 THz frequency range [15]. The broadband metamaterial absorber design is applicable in solar energy-harvesting photovoltaic devices [16]. Metamaterial absorbers are used in achieving broadband response, but still there is a room for improvement in the efficiency of these metamaterial solar absorbers.

Graphene metasurface solar absorbers are using graphene material which has excellent electrical and optical properties. These properties can be combined with graphene metasurface absorbers to design efficient and broadband solar absorbers. Graphene material is gaining interest in the researcher community because of its excellent properties ever since it has been invented [17]. Graphene gratings are used to reflect the waves coming on to the top surface of the gratings [18–20]. Graphene metasurface-based solar absorbers can be used to tune the frequency in terahertz region [21, 22]. Ultrafast lasers can also be designed using graphene-based absorbers [23]. Broadband absorbers are designed using different shape graphene metasurface [24–27]. The efficiency is important factor while designing any solar absorber. Graphene metasurface-based highly efficient solar absorber with broad-spectrum range is designed using gold resonators. The cost of such solar absorber is high because of its costly materials [28].

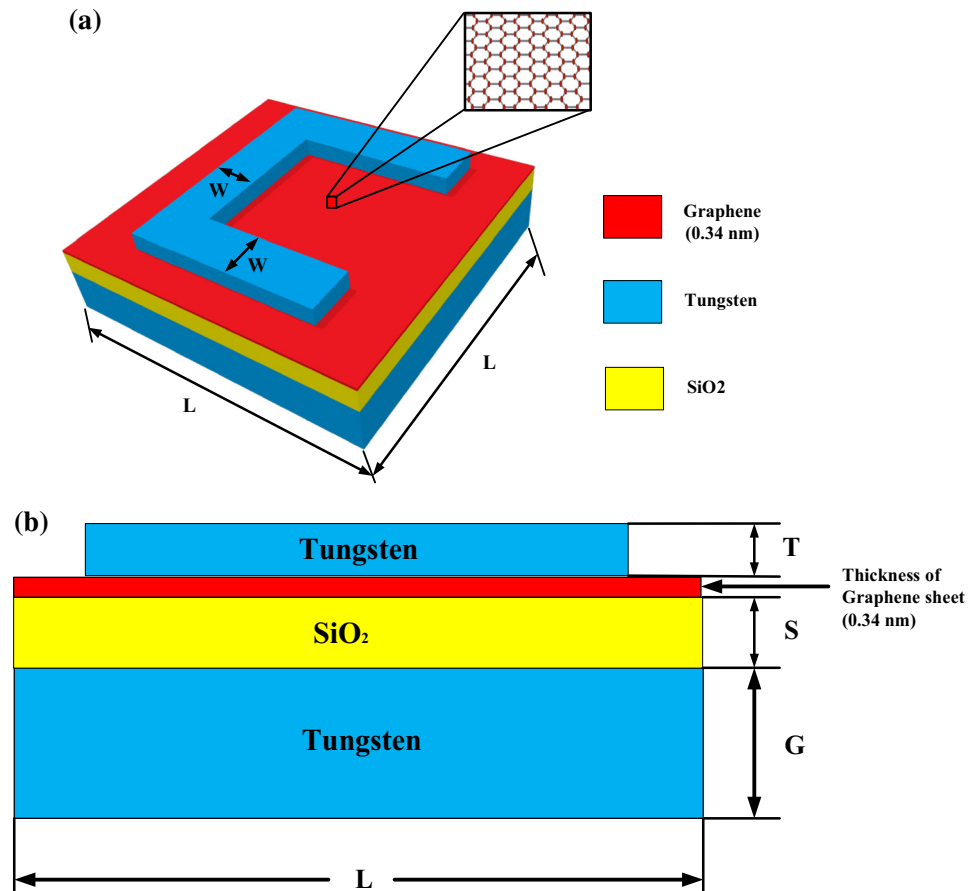
We have proposed that solar absorber is designed with tungsten material which costs less compared to the gold-based solar absorber. Our design is showing broadband response and high efficiency compared to previously published results, and the comparison is provided in results and discussion section. The proposed design is presented in “[Design and modelling](#)” section, and its results are presented and discussed in “[Results and discussions](#)” section.

Design and modelling

In this section, we presented our graphene metasurface-based solar absorber design. The three-dimensional design with its two-dimensional front view is presented in Fig. 1. Metasurface resonator made up of tungsten material is placed over graphene material. The graphene layer is placed over a SiO_2 spacer with tungsten substrate. The thickness (T) and width (W) of C-shape metasurface is 100 nm and 200 nm, respectively. The thickness of SiO_2 layer (S) and tungsten substrate (G) layer is kept at 300 nm and 600 nm, respectively. The thickness of these two layers is kept more so that there is more absorption and less transmittance through this layer. The total length of the structure is 2 μm .

The top metallic layer acts as a resonator. It generates resonance effect such that it helps in impedance matching condition. The dielectric medium

Figure 1 Graphene-based metasurface absorber design **a** three-dimensional design **b** two-dimensional design (front view). The top metasurface layer with the thickness (T) of 100 nm, width (W) of 200 nm and the bottom layer with the thickness (G) 600 nm. Both these layers are made up of tungsten material. The dielectric layer with the thickness (S) of 300 nm which separates the top and bottom layer is made up of SiO₂ material. The total length (L) of the structure is kept 2 μm .



layer helps to absorb the resonance frequency. The effectiveness of absorption is very important and is measured over here by the following equations [29]:

$$\Delta \times \vec{E} = i\omega\mu_0\vec{H} \quad (1)$$

$$\Delta \times \vec{H} = -i\omega\epsilon_0\epsilon\vec{E}$$

$$A(\omega) = \frac{Q_{\text{abs}}(\omega)}{Q_{\text{inc}}(\omega)} \quad (2)$$

$$Q_{\text{abs}} = \frac{\omega\epsilon_0}{2} \int_V \text{Im}[\epsilon(\omega)]|E|^2 dV \quad (3)$$

$$Q_{\text{abs}}^{\text{tot}} = \int A(\omega)F(\omega)d\omega \quad (4)$$

where Q_{abs} is spectral power absorbed by each element, $A(\omega)$ is optical absorption, $Q_{\text{abs}}^{\text{tot}}$ is total power absorbed and Q_{inc} is spectral power coming from the sun and incident on the solar surface. To achieve the maximum absorption, the bottom layer is added to reduce the reflection. The thickness of the bottom layer should be chosen more than the penetration depth of incident light to get minimum transmission

losses ($T(\omega) \approx 0$). The absorption $A(\omega)$ is very important parameter for the absorber design, and it is given by Eq. (5):

$$A(\omega) = 1 - R(\omega) - T(\omega) \quad (5)$$

$R(\omega)$ is reflection parameter and $T(\omega)$ is transmission parameter. All these three parameters (absorption, transmission and reflection) depend on frequency (ω). In addition, both $R(\omega)$ and $T(\omega)$ can be expressed in terms of S-parameters as $T(\omega) = |S_{21}|^2$ and $R(\omega) = |S_{11}|^2$.

The permittivity data of tungsten is adopted from [30]. The SiO₂ is a sandwich layer between the top and bottom layer with the thickness (S) of 300 nm and a refractive index experimental data is taken from [31]. The bottom layer (G) with a thickness of 600 nm helps in reducing the transmission of incoming incident electromagnetic wave. The monolayer sheet of graphene is added above the dielectric layer with length (L) of 2 μm . The thickness of the graphene sheet is considered as a 0.34 μm . The surface conductivity of infinite graphene sheet is given

by Kubo formula [32] presented in Eqs. (6–9). The total conductivity is the addition of intraband and interband conductivities as presented in the following equations.

$$\epsilon(\omega) = 1 + \frac{\sigma_s}{\epsilon_0 \omega \Delta} \tag{6}$$

$$\sigma_{\text{intra}} = \frac{-je^2 k_B T}{\pi \eta^2 (\omega - j2\Gamma)} \left(\frac{\mu_c}{k_B T} + 2 \ln \left(e^{\frac{-\mu_c}{k_B T}} + 1 \right) \right) \tag{7}$$

$$\sigma_{\text{inter}} = \frac{-je^2}{4\pi \hbar} \ln \left(\frac{2|\mu_c| - (\omega - j2\Gamma)\hbar}{2|\mu_c| + (\omega - j2\Gamma)\hbar} \right) \tag{8}$$

$$\sigma_s = \sigma_{\text{inter}} + \sigma_{\text{intra}} \tag{9}$$

The permittivity of graphene depends on the thickness of graphene monolayer sheet ($\Delta(0.34 \text{ nm})$), angular frequency (ω), surface conductivity (σ_s) and permittivity of vacuum (ϵ_0). Other such parameters in the equation of graphene surface conductivity (σ_s) also depend upon $k_B(1.38\text{e}^{-23} \text{ J/K})$ is the Boltzmann constant, temperature (T) in kelvin, $e(1.6\text{e}^{-19} \text{ C})$ is electron charge value, $\hbar(6.62\text{e}^{-34} \text{ J s})$ is the Planck’s constant, $\mu_c(0.3 \text{ eV})$ is chemical potential and also on electron–phonon, $\Gamma (11\text{e}^{-3} [1/\text{S}])$ is scattering rate. Graphene’s chemical potential is given by $\mu_c = \hbar V_F \sqrt{\pi C V_{DC} / e}$, V_{DC} is a gate voltage, C is the capacitance is given by $C = \epsilon_d \epsilon_0 / t$, t is dielectric layer thickness and ϵ_d is dielectric layer static permittivity. An electromagnetic plane wave is inserted normally from z -direction on proposed broadband absorber as shown in Fig. 1a.

Results and discussions

The proposed design presented in Fig. 1 is simulated using COMSOL Multiphysics, and the results in the form for absorption, electric field, etc., are presented in Figs. 2, 3, 4, 5, 6, 7 and 8. The design results are analysed by changing different physical parameters like width of resonator (W), thickness of resonator (T), thickness of SiO_2 layer (S) and height of substrate tungsten layer (T). The different physical parameters of the design are optimized to achieve broadband absorption in the visible region from 430 to 770 THz. The absorption result of the solar absorber is presented in Fig. 2 for 430 THz to 770 THz frequency range. The metasurface resonator and graphene layer placed above the dielectric layer collect all incoming light into a dielectric layer which leads to an increase

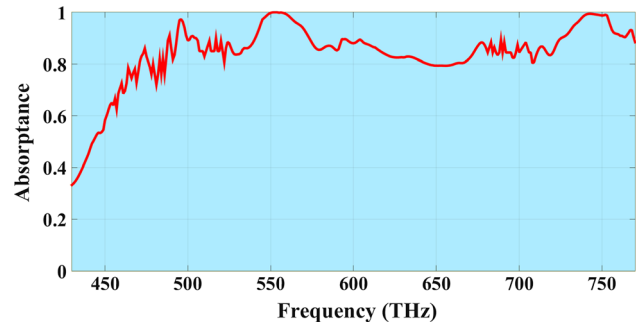


Figure 2 Absorption response of the proposed graphene-based metasurface solar absorber. The response of average absorption is 84% in the visible region from 430 to 770 THz. The absorption is near to unity for 550 THz and 750 THz frequencies.

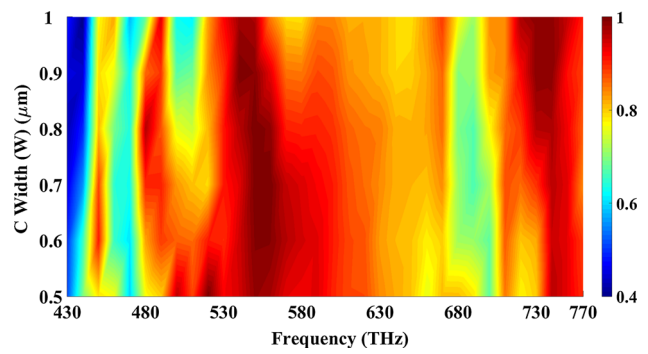


Figure 3 Graphene-based proposed solar absorber with a variation of metasurface width (W) from 0.5 to 1 μm . The red colour indicated the higher value, and blue colour indicate the lower value. The maximum absorption is achieved in the middle and end regions. The absorption decreases as the width of metasurface increases.

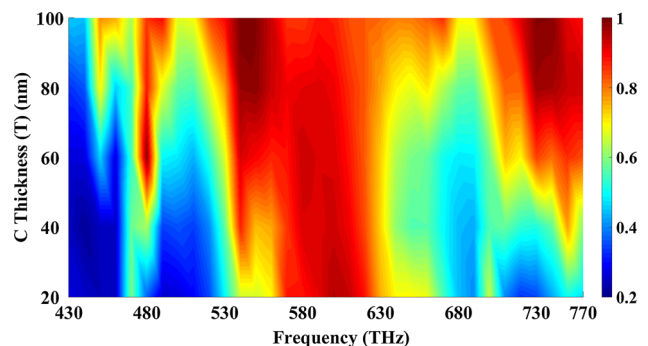


Figure 4 The graphene-based proposed solar absorber with a variation of C-shaped height (T) from 20 to 100 nm. The red colour indicates the higher value, and blue colour indicates the lowest value. From the graph, it has been observed that absorption decreases as the thickness of C-shaped decreases.

in absorption. The top layer and graphene layer reduce the reflection, and bottom tungsten layer is

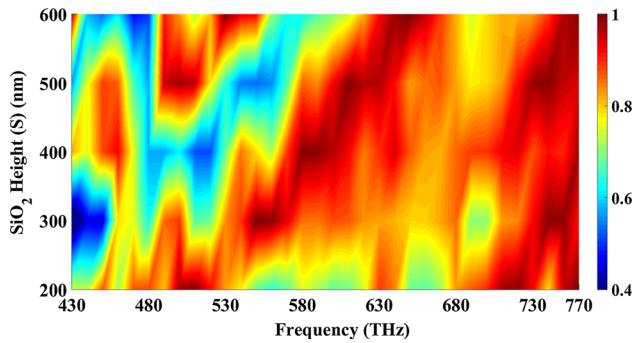


Figure 5 Graphene-based metasurface solar absorber with a variation of dielectric layer thickness (S) from 200 to 600 nm. The red colour indicates the higher value and blue colour indicates the lowest value. From the graph, it has been observed that absorption is more in the middle of the region between 290 and 450 nm.

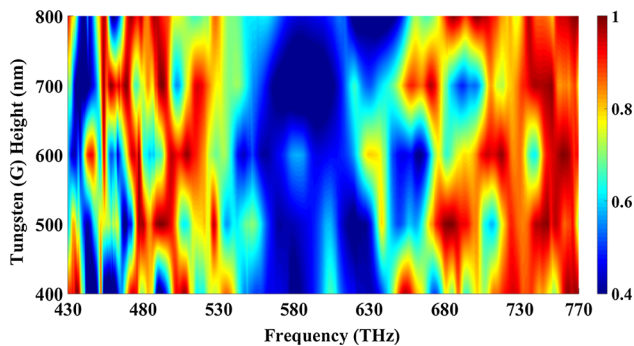


Figure 6 Graphene-based metasurface solar absorber with a variation of dielectric layer tungsten layer thickness (G) from 400 to 800 nm. The absorption is very weak for the middle frequency range of 535 THz to 635 THz. The increase in thickness also improves the absorption.

kept thick to reduce transmission, and thus, it doesn't allow light to pass through it. The optimized parameter of design leads to an average absorption of 84% in the visible region from 430 to 770 THz as shown in Fig. 2 (Table 1).

We vary the width (W) of metasurface layer from 0.5 to 1 μm to observe the effect on absorption in the visible region. As shown in Fig. 3, with increasing the width (W) of metasurface structure the gap of the C-Shape reduces, and it covers the whole region of the top layer and thus absorption decreases. It has been clearly observed that the absorption is more in the middle and end frequency region. It is because the peaks of resonator is around the same frequency range. The reflection increases as we increase the width (W) of C-shaped structure and results lead to decrease in absorption. The metasurface width (W) is

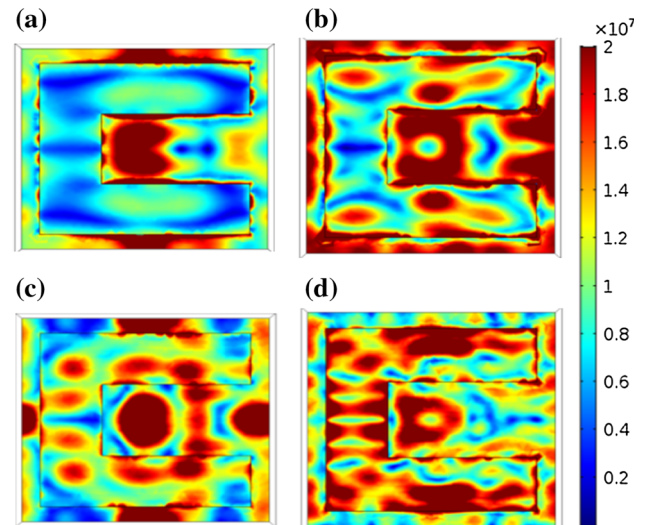


Figure 7 Electric field intensity for the frequency of **a** 430 THz, **b** 550 THz, **c** 650 THz, **d** 750 THz. The unit of the electric field is V/m; absorption is maximum on C-shaped metasurface made up tungsten.

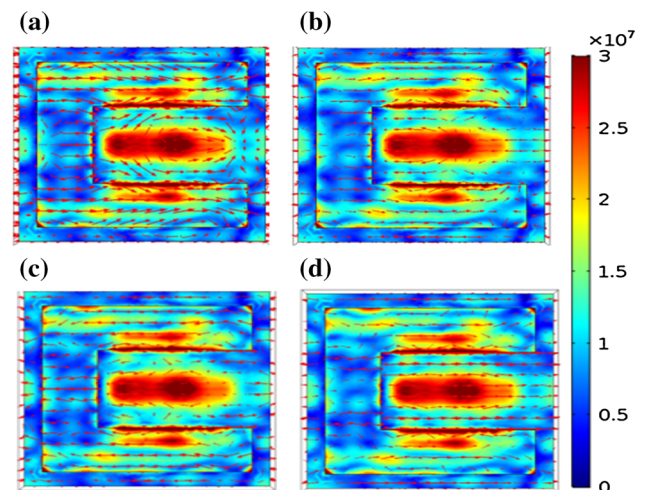


Figure 8 Magnetic field current density for the frequency of **a** 430 THz, **b** 550 THz, **c** 650 THz, **d** 750 THz. The unit of the magnetic field is A/m; the arrow in the figure indicates the current distribution which is more near metasurface elements.

varied from 0.5 to 1 μm , and frequency range is kept from 430 to 770 THz.

The top layer with C-shaped metasurface helps to improve absorption with minimum reflection at lower width values. The thickness (T) of C-shaped metasurface is varied from 20 to 100 nm by keeping all parameter constant to understand its effect on absorption in the visible region as shown in Fig. 4. The absorption increases as the thickness of C-shaped metasurface increases in the proposed design.

Table 1 Absorption efficiency comparison of proposed graphene-based metasurface solar absorber design with previously published solar absorber designs in the visible frequency range [24–26]

Solar absorber design	Absorption efficiency (%)
Proposed graphene-based metasurface tungsten solar absorber design	84
Design of Ref. [24]	71
Design of Ref. [25]	80
Design of Ref. [26]	70

The dielectric layer is responsible for the maximum absorption of incoming light into it. From Fig. 5, it is clearly indicated that when we change the thickness of the dielectric layer (S) from 200 to 600 nm, the absorption increases with increasing the thickness of the dielectric layer. This clearly shows that the thick layer (600 nm) absorbs more energy compared to the thin layer (200 nm). The absorption is also more for higher frequency values of 550 THz to 770 THz. The higher absorption in the layer increases the absorption efficiency of the absorber, and this high efficient absorber will be applicable in photovoltaic energy-harvesting devices.

The thickness of the bottom tungsten layer (G) also plays very important role in the absorption. The absorption for different tungsten layer thickness ranging from 400 to 800 nm and frequency range of 430 THz to 770 THz is presented in Fig. 6. From the results, it is clear that the increase in thickness improves the absorption to a certain extent. The middle frequency range of 535 THz to 635 THz has minimum absorption.

The results are also analysed to understand the effect of the electric field intensity and magnetic field current. The port of proposed graphene-based metasurface absorber is set to be a rectangular plot. The electromagnetic wave incident from port-1 of the structure and response is observed from port-2. The boundary condition is assigned in X – Y plane for a proposed three-dimensional graphene-based metasurface absorber design. We have presented the electric field intensity and magnetic field density at 430 THz, 550 THz, 650 THz and 750 THz in Figs. 7 and 8, respectively.

From the electric field intensity, it is clear that centre part of the absorber is absorbing the maximum electric energy as presented in Fig. 7. The energy is also increasing as we increase the frequency from

430 THz (Fig. 7a) to 750 THz (Fig. 7d). The results show that at 650 THz frequency maximum energy is concentrated in the absorber.

Magnetic field current density for different frequencies is presented in Fig. 8. Maximum concentration of magnetic field takes place at the central part, and this indicates maximum current density in that area. There is not much change in the current density by changing the frequency range from 430 to 750 THz. The arrows indicate the flow of current in the structure with its intensity is shown by different colours.

The proposed graphene-based metasurface absorber is giving broadband absorption in visible region which is better compared to the previously published designs. The tungsten material used for the solar absorber is very cost-effective material for designing solar absorbers.

Conclusion

In conclusion, a graphene-based broadband C-shaped metasurface absorber is proposed and the data are numerically investigated from 430 to 770 THz visible region of solar spectrum. The proposed design absorption band cover the whole visible region with an average absorption of 84%. The tunability in absorption peaks is obtained by varying the different physical parameters of the design like the thickness of C-shaped metasurface (T), the thickness of the dielectric layer (H) and width of metasurface (W) and thickness of tungsten layer (G). The absorption result decreases as we increase the metasurface thickness (T). The absorption decreases with the increase in the width of metasurface (W). Absorption increases with increase in the thickness of tungsten layer (G) and dielectric layer (H). The proposed design absorption efficiency is compared with the previously published design results. The proposed design results efficiency is showing great improvement over the other published results. The idea of using metasurface structure above the graphene sheet can be adopted for graphene-based optical devices, sensor and energy-harvesting devices.

Acknowledgement

Authors would like to acknowledge the support provided by Marwadi University, Rajkot and Ton Duc Thang University, Vietnam for this research.

Compliance with ethical standards

Conflict of interest The authors declare that they have no conflict of interest.

References

- [1] Zhang K, Hao L, Du M, Mi J, Wang JN, Meng JP (2017) A review of thermal stability and high temperature-induced ageing mechanisms of solar absorber coatings. *Renew Sust Energy Rev* 67:1282–1299
- [2] Tang L, Wu B, Tang P, Liu M, Zhan X, Liu X, Liu Z (2019) Silicon nano-cavity coupled metallic-dielectric colloidal crystals for narrow-band absorbers. *Opt Mater* 91:58–61
- [3] Liu N, Mesch M, Weiss T, Hentschel M, Giessen H (2010) Infrared perfect absorber and its application as plasmonic sensor. *Nano Lett* 10(7):2342–2348
- [4] Khan AD, Amin M (2017) Tunable Salisbury screen absorber using square lattice of plasmonic nanodisk. *Plasmonics* 12(2):257–262
- [5] Hsieh LZ, Chau YFC, Lim CM, Lin MH, Huang HJ, Lin CT, Syafii'e MIMN (2016) Metal nano-particles sizing by thermal annealing for the enhancement of surface plasmon effects in thin-film solar cells application. *Opt Commun* 370:85–90
- [6] McSherry S, Burger T, Lenert A (2019) Effects of narrow-band transport on near-field and far-field thermophotonic conversion. *J Photonics Energy* 9(3):032714
- [7] Li Q, Li Z, Xiang X, Wang T, Yang H, Wang X et al (2019) Tunable perfect narrow-band absorber based on a metal-dielectric-metal structure. *Coatings* 9(6):393
- [8] Cheng Y, Luo H, Chen F, Gong R (2019) Triple narrow-band plasmonic perfect absorber for refractive index sensing applications of optical frequency. *OSA Contin* 2(7):2113–2122
- [9] Ullah H, Khan AD, Ullah A, Ullah I, Noman M (2016) Plasmonic perfect absorber for solar cell applications. In: 2016 international conference on emerging technologies (ICET). IEEE, pp. 1–5
- [10] Hao J, Wang J, Liu X, Padilla WJ, Zhou L, Qiu M (2010) High-performance optical absorber based on a plasmonic metamaterial. *Appl Phys Lett* 96(25):251104
- [11] Kshetrimayum RS (2004) A brief intro to metamaterials. *IEEE Potentials* 23(5):44–46
- [12] Dang PT, Le KQ, Lee J-H, Nguyen TK (2019) A designed broadband absorber based on ENZ mode incorporating plasmonic metasurfaces. *Micromachines* 10(10):673
- [13] Nguyen TK, Dang PT, Park I, Le KQ (2017) Broadband THz radiation through tapered semiconductor grating on high-index substrate. *J Opt Soc Am B* 34(3):583–589
- [14] Patel SK, Charola S, Parmar J, Ladumor M (2019) Broadband metasurface solar absorber in the visible and near-infrared region. *Mater Res Lett* 6(8). <https://doi.org/10.1088/2053-1591/ab207d>
- [15] Katrodiya D, Jani C, Sorathiya V, Patel SK (2019) Metasurface based broadband solar absorber. *Opt Mater* 89:34–41
- [16] Bagmanci M, Karaaslan M, Unal E, Akgol O, Bakir M, Sabah C (2019) Solar energy harvesting with ultra-broadband metamaterial absorber. *Int J Mod Phys B* 33:1950056
- [17] Neto AC, Guinea F, Peres NM, Novoselov KS, Geim AK (2009) The electronic properties of graphene. *Rev Mod Phys* 81(1):109–162
- [18] Parmar J, Patel SK, Ladumor M, Sorathiya V, Katrodiya D (2019) Graphene-silicon hybrid chirped-superstructure bragg gratings for far infrared frequency. *Mater Res Lett* 6(6):065606
- [19] Patel SK, Ladumor M, Sorathiya V, Guo T (2018) Graphene based tunable grating structure. *Mater Res Lett* 6(2):025602
- [20] Patel SK, Ladumor M, Parmar J, Guo T (2019) Graphene-based tunable reflector superstructure grating. *Appl Phys A* 125(8):574
- [21] Chen M, Sun W, Cai J, Chang L, Xiao X (2017) Frequency-tunable terahertz absorbers based on graphene metasurface. *Opt Commun* 382:144–150
- [22] Yao Y, Shankar R, Kats MA, Song Y, Kong J, Loncar M, Capasso F (2014) Electrically tunable metasurface perfect absorbers for ultrathin mid-infrared optical modulators. *Nano Lett* 14(11):6526–6532
- [23] Bao Q, Zhang H, Wang Y, Ni Z, Yan Y, Shen ZX et al (2009) Atomic-layer graphene as a saturable absorber for ultrafast pulsed lasers. *Adv Funct Mater* 19(19):3077–3083
- [24] Sang T, Gao J, Yin X, Qi H, Wang L, Jiao H (2019) Angle-insensitive broadband absorption enhancement of graphene using a multi-grooved metasurface. *Nanoscale Res Lett* 14(1):105
- [25] Liu B, Tang C, Chen J, Xie N, Tang H, Zhu X, Park GS (2018) Multiband and broadband absorption enhancement of monolayer graphene at optical frequencies from multiple magnetic dipole resonances in metamaterials. *Nanoscale Res Lett* 13(1):153
- [26] Rufangura P, Sabah C (2017) Graphene-based wideband metamaterial absorber for solar cells application. *J Nanophotonics* 11(3):036008

- [27] Lin H, Sturmberg BC, Lin KT, Yang Y, Zheng X, Chong TK et al (2019) A 90-nm-thick graphene metamaterial for strong and extremely broadband absorption of unpolarized light. *Nat Photonics* 13(4):270–276
- [28] Patel SK, Charola S, Jani C, Ladumor M, Parmar J, Guo T (2019) Graphene-based highly efficient and broadband solar absorber. *Opt Mater* 96:109330
- [29] Akimov YA, Koh WS (2010) Resonant and nonresonant plasmonic nanoparticle enhancement for thin-film silicon solar cells. *Nanotechnology* 21(23):235201
- [30] Philipp HR (1997) Silicon dioxide(glass). In: Palik ED (ed) *Handbook of optical constants of solids*. Academic Press, Cambridge, pp 749–763
- [31] Palik ED (ed) (1998) *Handbook of optical constants of solids*, vol 3. Academic Press, Cambridge
- [32] Hanson GW (2008) Dyadic Green's functions and guided surface waves for a surface conductivity model of graphene. *Appl Phys* 103(6):064302

Publisher's Note Springer Nature remains neutral with regard to jurisdictional claims in published maps and institutional affiliations.